THE JOURNAL OF PHYSICAL CHEMISTRY Letters

Letter

pubs.acs.org/JPCL

Plasmon-Induced Conductance Enhancement in Single-Molecule Junctions

Michal Vadai,[†] Nirit Nachman,[†] Matan Ben-Zion,[†] Marius Bürkle,[‡] Fabian Pauly,[§] Juan Carlos Cuevas,[⊥] and Yoram Selzer*,[†]

[†]School of Chemistry, Tel Aviv University, Tel Aviv 69978, Israel

[‡]Institute of Theoretical Solid State Physics, Karlsruhe Institute of Technology, D-76131 Karlsruhe, Germany

[§]Department of Physics, University of Konstanz, D-78457 Konstanz, Germany

[⊥]Departamento de Física Teórica de la Materia Condensada and Condensed Matter Physics Center (IFIMAC), Universidad Autónoma de Madrid, E-28049 Madrid, Spain

Supporting Information

ABSTRACT: The effect of surface plasmons on the conductance of single-molecule junctions is studied using a squeezable break junction setup. We show that the conductance of 2,7-diaminofluorene single-molecule junctions can be enhanced upon laser irradiation. Our experimental approach enables us to show that this enhancement is due to the plasmon-induced oscillating field within the nanoscale metal gap of the junctions. The effective plasmon field enhancement within the gap is calculated to be ∼1000. The experimental procedure presented in this work, which enables one to explore the coupling between plasmons and molecular excitations via transport measurements, could potentially become a valuable tool in the field of plexcitonics.

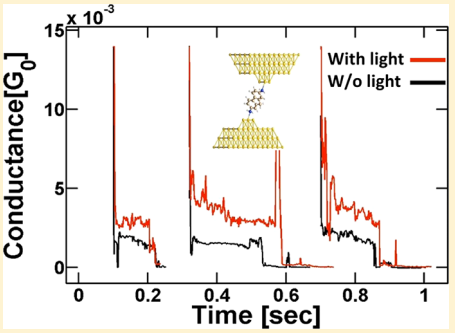

SECTION: Plasmonics, Optical Materials, and Hard Matter

Coherent oscillations of conduction electrons in a skin-layer of a metal, known as surface plasmons (SPs), are capable of concentrating light into deep subwavelength gaps between metallic nanostructured antennas with resulting electromagnetic field enhancement factors that can exceed 1000.[1−3] Such highly confined optical fields can efficiently mediate interactions between radiation and molecules residing in the gaps and have been utilized to develop surface-enhanced spectroscopy methods such as Raman,[4] IR absorption,[5] fluorescence,[6] and luminescence,[7] with a detection limit at the single-molecule level.

Plasmon coupling to molecular excitations[8] is studied in the field of plexcitonics.[9,10] Such couplings yield a possibility for the coherent control of molecular systems[11,12] and are utilized in molecular photodevices.[13−15] Plasmons are also predicted to generate, modulate, and steer charge-transfer processes through molecules by various mechanisms,[16] and several studies to demonstrate these effects have been published.[17−23] Yet, all of these works are based on either metallic atomic contacts or a large number of molecules in a relatively poorly defined junction geometry, analyzed with rather limited statistics. They are hence not sufficient to experimentally explore the next conceptual step in plexcitonics and nanoplasmonics, namely, a fully quantum mechanical treatment of the coupling between SPs and molecules and, more specifically, its effect on quantum transport through junctions.

Here, we report plasmon modulation of conductance in single-molecule junctions. Upon SP creation, a rectified dc current is formed in these junctions that is shown to be of optical origin, in this case, a photoassisted transport mechanism.[24,25] Other competing mechanisms can be excluded through our measurements. Considering the short duration time of plasmons in metals defined by the inverse of their spectral width $\Delta\omega^{-1}$ ($\hbar\Delta\omega \approx 2$ eV) and their short dephasing times of 10−100 fs,[26] our results are also an important step toward the possible realization of laser-controlled ultrafast molecular-scale electronics.

The geometry of junctions determines their near-field spectrum and the magnitude of the plasmonic field in their nanoscale gap.[27,28] Determination of this spectrum for setups such as the mechanically controlled or scanning tunneling microscope (STM) break junctions[29,30] is a difficult task,[31] especially because small variations in their structure could substantially change their plasmon resonance properties.[27,28] In addition, their poor heat dissipation characteristics may lead to the erroneous interpretation of changes in the conductance under illumination.[32]

To overcome these limitations, a squeezable break junction (SBJ) setup at room temperature and under ambient conditions

Received: July 7, 2013
Accepted: August 6, 2013

   dx.doi.org/10.1021/jz4014008 | J. Phys. Chem. Lett. 2013, 4, 2811−2816

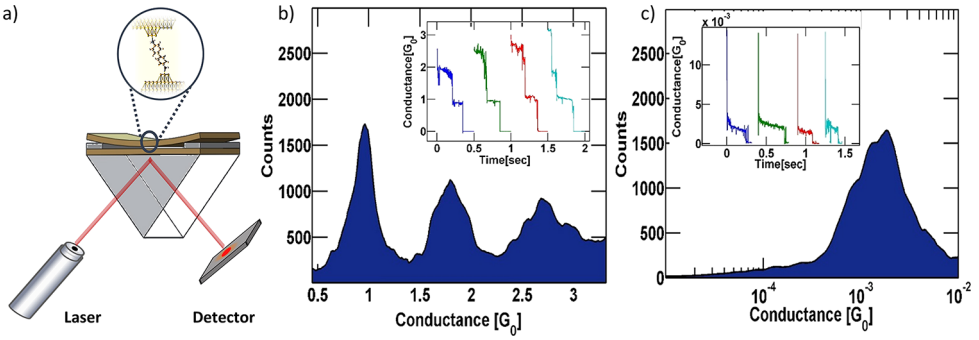

Figure 1. A SBJ setup for single-molecule conductance measurements. (a) Schematics of the experimental approach. Coupling between free photons and surface plasmons confined within the gap is established by a prism and by laser illumination in the total reflectance regime. (b) Conductance histogram of Au atomic contacts showing peaks around multiple integers of G_0. The inset shows typical conductance–time traces. (c) Conductance histogram for DAF molecular junctions with a peak at $1.86 \times 10^{-3} G_0$. Insets show the chemical structure of the molecule and typical conductance–time traces (note that the scale is in the mG_0 range). All measurements were carried out under a constant bias of 100 mV under ambient conditions.

has been used here. The SBJ consists of two 40 nm thick gold electrodes, 30 μm in width, evaporated on top of 1 mm BK7 glass slides with an initial gap of 500 nm in between, as displayed in Figure 1a. The gap can be mechanically controlled with high accuracy by applying a squeezing force against the top slide, allowing it to flex. Conductance traces are measured by squeezing the top slide until it contacts the bottom surface and then by measuring the conductance (typically at 0.1 V) while allowing the top slide to move back in steps of 10 pm. The dwell time in each step is typically 40 ms, although longer (up to 80 ms) and shorter (down to 10 ms) periods do not have any effect on the results. Conductance histograms are constructed from thousands of traces without any data selection or processing. Figure 1b depicts the obtained histogram for Au atomic contacts, revealing a quantized conductance with clear peaks around integer values of G_0, where $G_0 = 2e^2/h$ is the quantum of conductance. Thorough discussion on the possible reasons for deviation of the conductance values from exact integer multiplications of $1G_0$ can be found in ref 33. Because the SBJ is based on two Au-covered glass slides, measurements of single-atom contacts are made possible due to sufficient roughness of the Au surfaces. As will be shown below, this roughness is also essential for plasmon creation within the gap. Measurements of junctions with molecules are performed after a drop of solution (typically 1,2,4-trichlorobenzene) with <1 mM concentration of the molecule under test is applied to one of the Au surfaces before assembling the setup. Figure 1c shows a histogram measured with 2,7-diaminofluorene (DAF), revealing a molecular peak at $1.86 \times 10^{-3} G_0$, in agreement with a previously reported value.[29]

Creation of plasmons within the gap of the SBJ is achieved by an attenuated total reflection (Kretschmann) configuration,[34] by attaching a BK7 glass prism to the bottom slide (see Figure 1a) with a refractive index matching oil at the interface. Plasmon resonance conditions are found by varying θ, the angle of p-polarized light incident with respect to the surface normal, and by monitoring the intensity of the reflected light. All conductance measurements are performed at a θ corresponding to minimum reflectivity. The wavelength of the continuous-wave laser used in all experiments was 781 nm, the power was 10 mW, and the beam was focused to a spot with a radius of 80 μm. Maximum plasmon coupling is evidenced as a sharp drop in the reflectivity. At this point, a momentum matching condition is satisfied where the parallel component of the photon wave vector k_{light}, extended by the glass prism, matches that of a SP mode $k_{sp} = n \cdot k_{light} \cdot \sin\theta$. Here, n is the refractive index of the prism. In this configuration, plasmons are created only with a p-polarized (TM-mode) light.

The in-gap plasmon modes that are excited by this method are determined by calculating analytically the dispersion curves of an IMIMI (I, insulator; M, metal) geometry.[35] (The Supporting Information (SI) justifies why the SBJ setup can be approximated by this geometry.) Figure 2 shows three

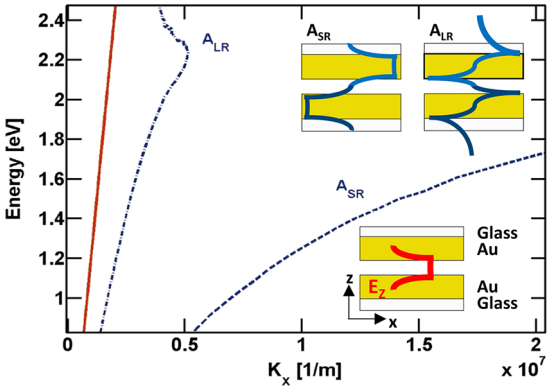

Figure 2. Analytic dispersion curves of an IMIMI configuration with 40 nm thick Au films and an inner 1 nm thick insulating layer of air. The red solid curve shows the dispersion for light within the prism (with an index of refraction of $n = 1.51$). The dispersions of two antisymmetric modes, the long-range mode A_{LR} and the short-range mode A_{SR}, are displayed as dashed–dotted and dashed curves, respectively. The profiles of E_x for these two modes are shown in the upper inset. The profile of E_z, the electric field component perpendicular to the interfaces, is similar for both and is shown in the lower inset.

curves relevant for our discussion here, the prism light line and the antisymmetric long-range (A_{LR}) and short-range (A_{SR}) modes. The latter two modes are characterized by a high field perpendicular to the interfaces and are localized within the junction gap. Because the prism light line resides at the left of A_{LR} and A_{SR}, no coupling between free photons and these modes is expected. However, this constraint is released in the presence of residual roughness of the Au surfaces with a periodicity a, which bridges the momentum mismatch by linearly adding $\Delta k = \pm 2\pi/a$ momentum vectors to the free photons.[34] Indeed, Fourier transforms of 2D correlation functions, calculated from atomic force microscopy images of

dx.doi.org/10.1021/jz4014008 | J. Phys. Chem. Lett. 2013, 4, 2811–2816

the 40 nm thick Au surfaces used in the SBJ setup, reveal a broad spectrum of Δk values that allow coupling between both in-gap SP modes and the prism light line (see the SI). This finding is on par with previous studies on prism-coupled light emission from tunnel junctions.[36]

Figure 3 summarizes the main results of this study. It compares histograms measured without laser illumination and

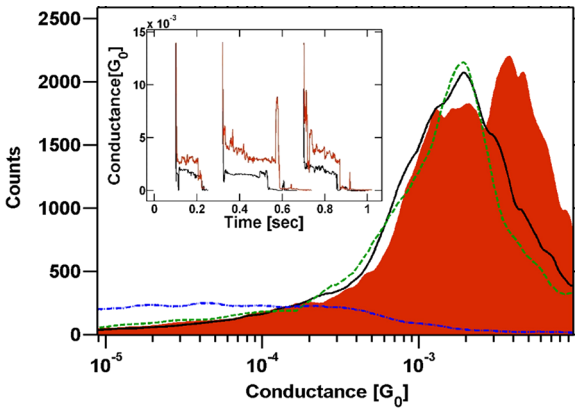

Figure 3. Effect of plasmons and light polarization on the conductance. Conductance histogram of DAF at 781 nm without illumination (black solid line), with p-polarized light for which plasmons are created (red colored area), and with s-polarized light for which no plasmons should be created (green dashed line). Additionally, a conductance histogram of the pure solvent (blue dashed line) is displayed with no apparent peaks. The histograms of the solvent with and without illumination are similar. (Inset) Representative conductance traces without (black) and with (red) laser illumination.

with s- and p-polarized continuous wave illumination. No effect of s-polarized light on the conductance is apparent as the histogram measured under these conditions is essentially identical to the histogram measured without light. In contrast, under p-polarized (TM-mode) illumination, a conductance peak appears at $3.7 \times 10^{-3} G_0$ above the characteristic peak without light. The appearance of this peak only under p-polarized illumination, that is, when plasmons can be created within the gap of the SBJ, supports their essential role in the apparent enhancement of the conductance. Further discussion on the reproducibility of the results can be found in the SI.

The fact that the conductance peak is not entirely shifted to a higher value under illumination can be rationalized in the following way. In each measurement of a conductance trace, as the two Au surfaces are separated, local hot spots are formed where momentum matching is achieved due to the local roughness, and local plasmons can be created. The short-range plasmon mode A_{SR}, which has the highest field within the gap (a factor of 10 larger than A_{LR}), possesses a propagation length, L_p, of a few tens of nanometers.[35,36] Hence, this plasmon can affect the conductance of a single molecule only if local roughness enables light coupling and plasmon creation within a distance of L_p from the molecule. Because this is not necessarily the case for all single-molecule measurement events, as each event probably takes place at a different location between the two opposing surfaces, only a fraction of the measurements is affected by plasmons, and the size of this fraction determines the intensity of the additional, higher-value conductance peak. It is also important to remember that the possibility to create plasmons at a certain location within the gap is subject to continuous change because during a set of measurements, the structure of the Au surfaces is constantly altered due to the repeated squeeze and release cycles.

Let us now try to elucidate the mechanism by which plasmons affect the conductance of the junctions. One possibility is lattice heating as a result of plasmon decay, which may lead to an enhanced conductance through hot molecules. In order to rule out this effect, the temperature in the junctions under illumination was measured by replacing one of the Au surfaces with a thin-film Au/Ag thermocouple. A maximal temperature increase of $\Delta T = 30$ K was determined at the plasmon resonance peak (see the inset of Figure 4 and the

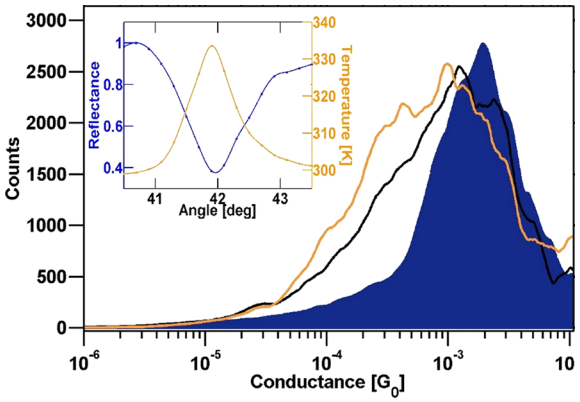

Figure 4. Effect of temperature on molecular conductance. Conductance histograms of molecular junctions with DAF measured at 300 (blue), 360 (black), and 380 K (orange). The molecular conductance peak at $1.86 \times 10^{-3} G_0$ is shifted to lower values as the temperature increases. The inset shows the temperature at the junction as a function of the incident angle under a 781 nm laser light (orange line) at 10 mW as determined by a calibrated thin-film thermocouple. The reflectance from the junction is shown as well (blue line). A maximum temperature increase of $\Delta T = 30$ K is achieved at the plasmonic resonance angle of 42°.

SI.) In contrast to the histograms in Figures 3 and S2 in the SI, Figure 4 shows that conductance histograms for molecular junctions of DAF, measured even at $\Delta T > 30$ K, exhibit an opposite effect to the one described above, that is, shifting of the peak to lower conductance accompanied by a broadening of the histogram. While further work is needed to fully understand this observation, the important conclusion for the discussion here is that lattice heating cannot be responsible for the conductance enhancement. In addition, we note that at temperatures higher than 380 K, the junctions were not stable enough to produce conductance histograms. This leads us to conclude that ΔT in the hot spots[37] and the local ionic effective temperature of the molecules in these locations cannot exceed 80 K.

Another mechanism that needs to be considered is a photothermoelectric effect, which arises when a temperature gradient, ΔT, across a junction is developed under illumination. This ΔT results in a thermovoltage $\Delta V_{TH} = -S\Delta T$, where S is the Seebeck coefficient of the junction. This parameter can be calculated from the transmission curve as a function of energy, $\tau(E)$, according to $S = -(\pi^2 k_B^2/3e)T(\partial \ln \tau(E)/\partial E)_{E=E_F}$, where k_B is the Boltzmann constant, e is the charge of an electron, and E_F is the Fermi energy.[38] From ab initio calculations (see the SI), we find that S is in the range of ~10 μV/K, which is on par with previously measured values.[38] The current through a

dx.doi.org/10.1021/jz4014008 | J. Phys. Chem. Lett. 2013, 4, 2811−2816

junction originating from the thermovoltage drop is $I_{TH} = G\Delta V_{TH}$, where G is the conductance of the junction. Using the experimental peak value for G (see Figure 1c) and $\Delta T = 30$ K (see the discussion above), the thermoelectric current is $I_{TH} <$ 0.1 nA. This is much smaller than the additional current that is measured through the junctions under illumination, which is on the order of several tens of nA. Hence, thermoelectric effects can be ruled out as well.

Another alternative explanation for the observed results would be an enhanced probability to measure more than one molecule upon illumination. There are essentially two mechanisms by which junctions with multiple molecules would become more favorable under illumination, namely, either by thermal activation of molecular fluctuations or by plasmonic field alignment of the molecules.[39,40] The first mechanism is ruled out by the experiments performed with external heating (see Figure 4) as heating appears to decrease and broaden the conductance distribution. The second mechanism is ruled out by considering theoretical calculations of molecular (plasmonic) field alignment,[39,40] which show that the required local electromagnetic field for molecular alignment exceeds the one present in our junctions by a factor of (at least) 1000 (see the detailed discussion below).

We also note that the width of the plasmon-induced peak is similar to the width of the conductance peak in the absence of light. This further supports our assertion that the number of molecules in the junction is unchanged because the width of a two-molecule peak should also be wider than that of a single-molecule peak.[41]

Finally, we also rule out the possibility that the enhanced conductance is due to photon absorption by the molecules within the junctions.[16] This is based on the fact that, as will be discussed further below, the HOMO−LUMO energy gap of DAF (>3 eV) is larger than the energy of the created plasmons (1.59 eV).

Let us now discuss a mechanism that is consistent with our observation of conductance enhancement in the junctions. Under conditions where electronic excitations within the molecule can be disregarded, the effect of the plasmonic oscillating field on the conductance of the junctions can be analyzed by invoking the Tien-Gordon model, that is, by considering a time-dependent modulation of the electronic energies.[42] In this model, the plasmon field is treated as a potential, V_ω, across the nanoscale gap, which oscillates at the plasmon frequency ω. An electron tunneling through the junction with initial energy E can either absorb or emit n photons with energy $\hbar\omega$ and hence finish the tunneling process at energy $E \pm \hbar\omega$. The probability for each of these events depends on $J_n^2(\alpha)$, the square of the Bessel function of order n evaluated at $\alpha = eV_\omega/\hbar\omega$. As a result, the transmission probability of an electron across a junction becomes $\tau(E) \rightarrow \sum_{n=-\infty}^{n=\infty} J_n^2(\alpha)\tau(E + n\hbar\omega)$, and the overall dc conductance of a junction at the Fermi energy E_F is described by

$$G_{dc}(\omega) = G_0 \sum_{n=-\infty}^{n=\infty} J_n^2(\alpha)\tau(E_F + n\hbar\omega) \quad (1)$$

The transmission (E) is determined by the molecule and its coupling to the leads.

Another (perhaps more intuitive) way to understand this mechanism is as if V_ω acts like a gate that shifts $\tau(E)$ up and down by integer values of $\hbar\omega$, where for each shift, a different portion of $\tau(E)$ is located within the energy window defined by the applied voltage bias, where transport takes place.

Using this model, the observed conductance enhancement can be rationalized with the help of eq 1 and the transmission curve shown in Figure 5, which was computed by a transport method[43] that is based on density functional theory (DFT) (see the SI for more details) and was calculated for a stable configuration of a DAF-based Au junction.

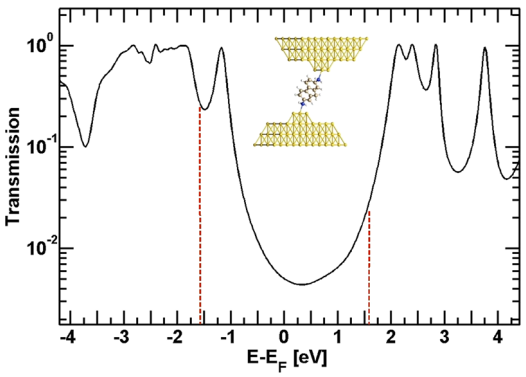

Figure 5. Theoretical zero-bias transmission as a function of energy for DAF in Au junctions. The vertical dashed lines are positioned at ±1.59 eV (λ = 781 nm) above and below the Fermi energy, indicating the change in transmission for an electron that interacts inelastically with the oscillating potential V_ω within the gap by either absorbing or emitting one photon. The conductance enhancement is dominated by electrons that undergo the latter process as the transmission above the Fermi level is much smaller for the wavelength used. The inset shows the studied contact geometry.

In the optical range, eV_ω is expected to be much smaller than the photon energy $\hbar\omega$, and in this limit, eq 1 reduces to

$$G_{dc}(\omega) - G_{dc}(\omega = 0) = \left(\frac{eV_\omega}{2\hbar\omega}\right)^2 G_0\{\tau(E_F + \hbar\omega) + \tau(E_F - \hbar\omega) - 2\tau(E_F)\} \quad (2)$$

In view of the energy dependence of the transmission (see Figure 5), $\tau(E_F - \hbar\omega) \gg \tau(E_F + \hbar\omega), \tau(E_F)$. Therefore, on the basis of eq 2, it is clear that the conductance is enhanced upon illumination mainly due to single-photon emission tunneling processes, coupling the Fermi energy with the region below the HOMO.

Ignoring the contribution of $\tau(E_F + \hbar\omega)$ and $\tau(E_F)$, eq 2 can be further simplified to

$$eV_\omega = 2\hbar\omega\sqrt{\frac{G_{dc}(\omega) - G_{dc}(0)}{G_0\tau(E_F - \hbar\omega)}} \quad (3)$$

and subsequently be used in order to estimate the plasmonic field enhancement within the junctions.[17,20−22]

On the basis of the experimental value of $G_{dc}(\omega) - G_{dc}(0)$ and the theoretical value of $\tau(E_F - \hbar\omega)$, V_ω is determined to be 0.169 V. In order to estimate the error in this value, we note that based in Figure 5, $\tau(E)$ typically takes a value close to 1 below the HOMO and varies between 0.1 and 1 in a large energy range of 3 eV below it. Due to the square root in eq 3, V_ω varies only within a factor of 3 when the transmission changes by 1 order of magnitude. Hence, as long as the transport at $E = E_F - \hbar\omega$ remains on-resonance, the oscillating potential V_ω is rather insensitive to variations of the precise

dx.doi.org/10.1021/jz4014008 | J. Phys. Chem. Lett. 2013, 4, 2811−2816

shape of the transmission curve as they could arise from inaccuracies of the DFT method or changes in the junction structure. Further discussion on this issue can be found in the SI.

With the above V_ω and considering the light intensity and the penetration depth of Au at 781 nm (~1 nm),[44] the corresponding plasmonic field enhancement factor is 1100. This value is consistent with recent theoretical estimations,[44] previous measurements of rectification currents in subnanometer gap junctions,[17] and surface-enhanced Raman measurements.[45]

An alternative mechanism to explain the observed plasmon-induced conductance enhancement is by generation of hot electrons in the metal electrodes via plasmon decay.[46] In the SI, we show analytically that, to lowest order in α ($\alpha = eV_\omega/\hbar\omega$), this process is described by eq 1. Hence, for the laser intensity used here, the two mechanisms are identical.

In conclusion, we show the effect of plasmons on single-molecule junctions, demonstrated in this study as an enhanced dc conductance. The novel experimental setup enables one to rule out the contribution of other processes that could enhance the conductance upon laser illumination, leaving only the optical plasmonic field as the source of the measured effect. Because pulsed lasers offer the possibility to create rapid (femtosecond and below) transient plasmons, the demonstrated experimental capability opens a path to ultrafast (optical) gating of single-molecule junctions toward the realization of new nanoscale electronics faster than current technology by several orders of magnitude.

■ ASSOCIATED CONTENT

Supporting Information

Details on experimental procedures, ab initio calculations, and the accuracy and robustness of extracted parameters. This material is available free of charge via the Internet at http://pubs.acs.org.

■ AUTHOR INFORMATION

Corresponding Author

*E-mail: selzer@post.tau.ac.il.

Notes

The authors declare no competing financial interest.

■ ACKNOWLEDGMENTS

M.B. acknowledges support through the DFG Priority Program 1243 as well as the DFG Center for Functional Nanostructures (Project C3.6), and F.P. acknowledges support through the Carl-Zeiss Foundation and the SFB 767. J.C.C. thanks the Institute for Advanced Studies of the Hebrew University of Jerusalem for the hospitality during the workshop on molecular electronics. M.V. wishes to thank L. Wang and Q. Gong from Peking University for valuable help in the calculations of the dispersion curves. Y.S. thanks the ISF (both the usual track and F.I.R.S.T), the GIF, and the Wolfson foundation for renewable energy research for financial support.

■ REFERENCES

(1) Novotny, L.; van Hulst, N. Antennas for Light. *Nat. Photonics* **2011**, *5*, 83−90.

(2) Mühlschlegel, P.; Eisler, H.-J; Martin, O. J. F.; Hecht, B.; Pohl, D. W. Resonant Optical Antennas. *Science* **2005**, *308*, 1607−1609.

(3) Schuck, P. J.; Fromm, D. P.; Sundaramurthy, A.; Kino, G. S.; Moerner, W. E. Improving the Mismatch Between Light and Nanoscale Objects with Gold Bowtie Nanoantennas. *Phys. Rev. Lett.* **2005**, *94*, 017402.

(4) Kleinman, S. L.; Ringe, E.; Valley, N.; Wustholtz, K. L.; Phillips, E.; Scheidt, K. A.; Schatz, G. C.; Van Duyne, R. P.. Single-Molecule Surface-Enhanced Raman Spectroscopy of Crystal Violet Isotopologues: Theory and Experiment. *J. Am. Chem. Soc.* **2011**, *133*, 4115−4122.

(5) Adato, R.; Yanik, A. A.; Amsden, J. J.; Kaplan, D. L.; Omenetto, F. G.; Hong, M. K.; Erammilli, S.; Altug, H. Ultra-sensitive Vibrational Spectroscopy of Protein Monolayers with Plasmonic Nanoantenna Arrays. *Proc. Natl. Acad. Sci. U.S.A.* **2009**, *106*, 19227−19232.

(6) Kinkhabwala, A.; Yu, Z.; Fan, S.; Avlasevich, Y.; Mülen, K.; Moerner, W. E. Large Single-Molecule Fluorescence Enhancements Produced by a Bowtie Nanoantenna. *Nat. Photonics* **2009**, *3*, 654−657.

(7) Dong, Z. C.; Zhang, X. L.; Gao, H. Y.; Lou, Y.; Zhang, C.; Chen, L. G.; Zhang, R.; Tao, X.; Zhang, Y.; Yang, J. L.; Hou, J. G. Generation of Molecular Hot Electroluminescence by Resonant Nanocavity Plasmons. *Nat. Photonics* **2010**, *4*, 50−54.

(8) Zhang, Q.; Atay, T.; Tischler, J. R.; Bradley, M. S.; Bulovic, V.; Nurmikko, A. V. Highly Efficient Resonant Coupling of Optical Excitations in Hybrid Organic/Inorganic Semiconductor Nanostructures. *Nat. Nanotechnol.* **2007**, *2*, 555−559.

(9) Fofang, N. T.; Park, T.-H.; Neumann, O.; Mirin, N. A.; Nordlander, P.; Halas, N. J. Plexcitonic Nanoparticles: Plasmon−Exciton Coupling in Nanoshell−J-Aggregate Complexes. *Nano Lett.* **2008**, *8*, 3481−3487.

(10) White, A. J.; Fainberg, B. D.; Galperin, M. Collective Plasmon-Molecule Excitations in Nanojunctions: Quantum Consideration. *J. Phys. Chem. Lett.* **2012**, *3*, 2738.

(11) Wiederrecht, G. P.; Wurtz, G. A.; Hranisavljevic, J. Coherent Coupling of Molecular Excitons to Electronic Polarizations of Noble Metal Nanoparticles. *Nano Lett.* **2004**, *4*, 2121−2125.

(12) Wurtz, G. A.; Evans, P. R.; Hendren, W.; Atkinson, R.; Dickson, W.; Pollard, R. J.; Zayats, A. V.; Harrison, W.; Bower, C. Molecular Plasmonics with Tunable Exciton−Plasmon Coupling Strength in J-Aggregate Hybridized Au Nanorod Assemblies. *Nano Lett.* **2007**, *7*, 1297−1303.

(13) Eisele, D. M.; Knoester, J.; Kirstein, S.; Rabe, J. P.; Vanden Bout, D. A. Uniform Exciton Fluorescence from Individual Molecular Nanotubes Immobilized on Solid Substrates. *Nat. Nanotechnol.* **2009**, *4*, 658−663.

(14) Walker, B. J.; Dorn, A.; Bulovic, V.; Bawendi, M. G. Color-Selective Photocurrent Enhancement in Coupled J-Aggregate/Nanowires Formed in Solution. *Nano Lett.* **2011**, *11*, 2655−2659.

(15) Zheng, Y. B.; Kiraly, B.; Cheunkar, S.; Huang, T. J.; Weiss, P. S. Incident-Angle-Modulated Molecular Plasmonic Switches: A Case of Weak Exciton−Plasmon Coupling. *Nano Lett.* **2011**, *11*, 2061−2065.

(16) Galperin, M.; Nitzan, A. Molecular Optoelectronics: The Interaction of Molecular Conduction Junctions with Light. *Phys. Chem. Chem. Phys.* **2012**, *14*, 9421−9438.

(17) Ward, D. R.; Hüser, F.; Pauly, F.; Cuevas, J. C.; Natelson, D. Optical Rectification and Field Enhancement in a Plasmonic Nanogap. *Nat. Nanotechnol.* **2010**, *5*, 732−736.

(18) Mangold, M. A.; Calame, M.; Mayor, M.; Holleitner, A. W. Resonant Photoconductance of Molecular Junctions Formed in Gold Nanoparticle Arrays. *J. Am. Chem. Soc.* **2011**, *133*, 12185−12191.

(19) Guhr, D. C.; Rettinger, D.; Boneberg, J.; Erbe, A.; Leiderer, P.; Scheer, E. Influence of Laser Light on Electronic Transport Through Atomic-Size Contacts. *Phys. Rev. Lett.* **2007**, *99*, 086801.

(20) Noy, G.; Ophir, A.; Selzer, Y. Response of Molecular Junctions to Surface Plasmon Polaritons. *Angew. Chem., Int. Ed.* **2010**, *49*, 5734−5736.

(21) Ittah, N.; Selzer, Y. Electrical Detection of Surface Plasmon Polaritons by $1G_0$ Gold Quantum Point Contacts. *Nano Lett.* **2011**, *11*, 529−534.

(22) Arielly, R.; Ofarim, A.; Noy, G.; Selzer, Y. Accurate Determination of Plasmonic Fields in Molecular Junctions by Current Rectification at Optical Frequencies. *Nano Lett.* **2011**, *11*, 2968−2972.

(23) Banerjee, P.; Conklin, D.; Nanayakkara, S.; Park, T.-H.; Therien, M. J.; Bonnell, D. A. Plasmon-Induced Electrical Conduction in Molecular Devices. *ACS Nano* **2010**, *4*, 1019−1025.
(24) Viljas, J. K.; Cuevas, J. C. Role of Electronic Structure in Photoassisted Transport through Atomic-Sized Contacts. *Phys. Rev. B* **2007**, *75*, 075406.
(25) Viljas, J. K.; Pauly, F.; Cuevas, J. C. Photoconductance of Organic Single-Molecule Contacts. *Phys. Rev. B* **2007**, *76*, 033403.
(26) MacDonald, K. F.; Samson, Z. L.; Stockman, M. I.; Zheludev, N. I. Ultrafast Active Plasmonics. *Nat. Photonics* **2009**, *3*, 55−58.
(27) Yang, Y.; Zhang, Y. L.; Jin, F.; Dong, X. Z.; Duan, X. M.; Zhao, Z. S. Steering the Optical Response with Asymmetric Bowtie 2-Color Controllers in the Visible and Near Infrared Range. *Opt. Commun.* **2011**, *284*, 3474−3478.
(28) García-Martín, A.; Ward, D. R.; Natelson, D.; Cuevas, J. C. Field Enhancement in Subnanometer Metallic Gaps. *Phys. Rev. B* **2011**, *83*, 193404.
(29) Venkataraman, L.; Klare, J. E.; Nuckolls, C.; Hybertsen, M. S.; Steigerwald, M. L. Dependence of Single-Molecule Junction Conductance on Molecular Conformation. *Nature* **2006**, *442*, 904−907.
(30) Martin, C. A.; Smit, R. H. M.; van Egmond, R.; van der Zant, H. S. J.; van Ruitenbeek, J. M. A Versatile Low Temperature Setup for the Electrical Characterization of Single Molecule Junctions. *Rev. Sci. Instrum.* **2011**, *82*, 053907.
(31) Jiang, N.; Foley, E. T.; Klingsporn, J. M.; Sonntag, M. D.; Valley, N. A.; Dieringer, J. A.; Seideman, T.; Schatz, G. C.; Hersam, M. C.; Van Duyne, R. P. Observation of Multiple Vibrational Modes in Ultrahigh Vacuum Tip-Enhanced Raman Spectroscopy Combined with Molecular-Resolution Scanning Tunneling Microscopy. *Nano Lett.* **2012**, *12*, 5061−5067.
(32) Grafstrom, S.; Kowalski, J.; Neumann, R.; Probst, O.; Wortge, M. Analysis and Compensation of Thermal Effects in Laser-Assisted Scanning Tunneling Microscopy. *J. Vac. Sci. Technol., B* **1991**, *9*, 568−572.
(33) Agrait, N.; Levy Yeyati, A.; van Ruitenbeek, J. M. Quantum Properties of Atomic-Sized Conductors. *Phys. Rep.* **2003**, *377*, 81.
(34) Raether, H. *Surface Plasmons on Smooth and Rough Surfaces and on Gratings*; Springer Tracts in Modern Physics; Springer: Berlin, Germany, 1988; Vol. *111*.
(35) Wang, L.; Gu, Y.; Hu, X.; Gong, Q. Long-Range Surface Plasmon Polariton Modes with a Large Field Localized in a Nanoscale Gap. *Appl. Phys. B: Laser Opt.* **2011**, *104*, 919−924.
(36) Ushioda, S.; Rutledge, J. E.; Pierce, R. M. Prism-Coupled Light Emission from Tunnel Junctions. *Phys. Rev. Lett.* **1985**, *54*, 224−226.
(37) Alessandri, I.; Ferroni, M.; Depero, L. E; In Situ Plasmon-Heating-Induced Generation of Au/TiO_2 "Hot Spots" on Colloidal Crystals. *ChemPhysChem* **2009**, *10*, 1017−1022.
(38) Reddy, P.; Jang, S. Y.; Segalman, R. A.; Majumdar, A. Thermoelectricity in Molecular Junctions. *Science* **2007**, *315*, 1568−1571.
(39) Reuter, M. G.; Ratner, M. A.; Seideman, T. Laser Alignment as a Route to Ultrafast Control of Electron Transport through Junctions. *Phys. Rev. A* **2012**, *86*, 013426.
(40) Artamonov, M.; Seideman, T. Predicted Ordered Assembly of Ethylene Molecules Induced by Polarized Off-Resonance Laser Pulses. *Phys. Rev. Lett.* **2012**, *12*, 168302.
(41) Reuter, M. G.; Hersam, M. C.; Seideman, T.; Ratner, M. A. Signatures of Cooperative Effects and Transport Mechanisms in Conductance Histograms. *Nano Lett.* **2012**, *12*, 2243.
(42) Tien, P. K.; Gordon, J. P. Multiphoton Process Observed in the Interaction of Microwave Fields with the Tunneling between Superconductor Films. *Phys. Rev.* **1963**, *129*, 647−651.
(43) Pauly, F.; Viljas, J. K.; Huniar, U.; Häfner, M.; Wohlthat, S.; Bürkle, M.; Cuevas, J. C.; Schön, G. Cluster Based Density-Functional Approach to Quantum Transport through Molecular and Atomic Contacts. *New J. Phys.* **2008**, *10*, 125019−125047.
(44) Ciraci, C.; Hill, R. T.; Mock, J. J.; Urzhumov, Y.; Fernandez-Dominguez, A. I.; Maier, S. A.; Pendry, J. B.; Chilkoti, A.; Smith, D. R. Probing the Ultimate Limits of Plasmonic Enhancement. *Science* **2012**, *337*, 1072−1074.
(45) Kneipp, K.; Wang, Y.; Kneipp, H.; Perelman, L. T.; Itzkan, I.; Dasari, R. R.; Feld, M. S. Single Molecule Detection Using Surface-Enhanced Raman Scattering (SERS). *Phys. Rev. Lett.* **1997**, *78*, 1667−1670.
(46) Sobhani, A.; Knight, M. W.; Wang, Y.; Zheng, B.; King, N. S.; Brown, L. V.; Fang, Z.; Nordlander, P.; Halas, N. J. Narrowband Photodetection in the Near-Infrared with a Plasmon-Induced Hot Electron Device. *Nat. Commun.* **2013**, *4*, 1643−1647.